

Structure based drug repurposing through targeting Nsp9 replicase and Spike Proteins of SARS-CoV-2

Vaishali Chandel¹, Prem Prakash Sharma², Sibi Raj¹, Brijesh Rathi², Dhruv Kumar^{1,*}

¹Amity Institute of Molecular Medicine & Stem Cell Research (AIMMSCR), Amity University Uttar Pradesh, Sec-125, Noida-201313, India

²Laboratory for Translational Chemistry and Drug Discovery, Department of Chemistry, Hansraj College, University of Delhi, Delhi-110007 India

*Corresponding Author: Dr. Dhruv Kumar, J3-112, Amity Institute of Molecular Medicine & Stem Cell Research (AIMMSCR), Amity University Uttar Pradesh, Sec-125, Noida-201313, India Tel: 7082436598

Email: dhruvbhu@gmail.com, dkumar13@amity.edu

Abstract

Due to unavailability of therapeutic approach for the novel coronavirus disease (COVID-19), the drug repurposing approach would be the fastest and efficient way of drug development against this deadly disease. We have applied bioinformatics approach for structure-based drug repurposing to identify the potential inhibitors through drug screening, molecular docking and molecular dynamics against non-structural protein 9 (Nsp9) replicase and spike proteins of the SARS-CoV-2 from the FDA approved drugs. We have performed virtual screening of 2000 FDA approved compounds including antiviral, anti-malarial, anti-parasitic, anti-fungal, anti-tuberculosis and active phytochemicals against Nsp9 replicase and spike proteins of SARS-CoV-2. Molecular docking was performed using Autodock-Vina. Selected hit compounds were identified based on their highest binding energy and favourable ADME profile. Notably, Conivaptan, an arginine vasopressin antagonist drug exhibited highest binding energy (-8.4 Kcal/mol) and maximum stability with the amino acid residues present on the active site of Nsp9 replicase. Additionally, Tegobuvir, a non-nucleoside inhibitor of hepatitis C virus exhibited maximum stability with highest binding energy (-8.1 Kcal/mol) on the active site of spike protein. Molecular docking scores were further validated with the molecular dynamics using Schrodinger, which supported strong stability of ligands with proteins at their active site through water bridges, hydrophobic interactions, H-bond. Overall, our findings highlight the fact that Conivaptan and Tegobuvir could be used to control the infection and propagation of SARS-CoV-2 targeting Nsp9 replicase and spike protein, respectively. Moreover, *in vitro* and *in vivo* validation of these findings will be helpful in bringing these molecules at the clinical settings.

Key words: COVID-19, SARS-CoV-2, Nsp9 replicase, spike protein, molecular docking, drug designing, drug repurposing

Introduction

Today, coronavirus created an alarming situation across the globe causing deaths more than million people. Origin studies of COVID-19 stated that it was closely related to the bat severe acute respiratory syndrome coronavirus 2 (SARS-CoV-2). Coronaviruses (CoVs) are the enveloped virus which comes under the family of coronaviridae with a positive sense single-stranded RNA genome [1]. The genome size of CoVs are large in size which ranges from approximately 27 to 37 kilobases. The envelope of the virus contains the lipid bilayer with three structural proteins membrane (M), envelope (E), and spike (S) [2]. The nucleocapsid protein present in multiple copy is associated along with the positive sense single stranded RNA genome and is responsible for the formation of nucleocapsid present inside the envelope. Viral protection outside host is delivered by the lipid bilayer, nucleocapsid and the membrane proteins. The CoV infection is attained via the S glycoprotein which attaches to the complementary host receptor. The entry of viral particles and its attachment to host membrane is mediated via direct fusion of the viral envelope or via endocytosis with the host membrane [3]. Since CoVs have single positive stranded RNA genome, CoVs are capable of producing required new genomes and proteins into the cytoplasm. Polymerase is synthesized by the virus itself and this polymerase further synthesizes the minus strand using the positive strand as template. This positive sense genomic RNA generated through replication is used its own genome in progeny viruses. The genomic RNA is attached with the N glycoprotein and further M glycoprotein integrates into the endoplasmic reticulum membrane exactly as the S and HE proteins. ER is the source for the translation of RNA and viral structural proteins. The M protein here assists the protein-protein interactions that helps in the assembly of viral particles followed by its binding to nucleocapsid. These are then released from the host cell via exocytosis [4]. Main protease domain (Mpro) has been reported to be a conserved target, in favour to design new inhibitors throughout the entire coronaviridae subfamily. The two-third

region of 5' in the coronavirus genome consists of the of open reading frame I (ORFI) which encodes two large polypeptides involved in the replicase machinery: pp1a, and via ribosomal frameshift, pp1ab1. Two proteases encoded in the 5' region of ORF 1: 3C-like protease (3CL or Nsp5) and papain-like protease (PLP) co-translationally cleaves the two polypeptides into mature non-structural proteins (NSPs) [5]. 3CL protease is also majorly called as Mpro as it has a dominant role in the post-translational machinery of the replicase protein. Significant homology of Mpros in primary amino acid sequence as well as in 3D architecture has been reported in different human and animal CoVs. Both of these proteins have a substrate binding pocket where at P1 glutamine is the substrate and at the P2 either leucine or methionine. This strong structural basis provides a loop hole to design a wide-spectrum anti CoV inhibitors. In general, there are few or no treatment options for viral diseases that occur suddenly and spread at a higher frequency.

The spike proteins crowing the novel virus has been of major research interest as to know how they attach, fuse and gain entry to the host cell. There are mainly two subunits of the spike protein, namely S1 and S2 subunits. The S1-portion has diverged sequences even among single coronavirus species whereas, the S2 subunit is the most conserved area. The S1 subunit has 2 domains N and C terminal domains. These domains mainly function as receptor binding domains and binds themselves to various proteins and sugar molecules. These spike proteins contain heptad repeats of hydrophobic domains that helps in the fusion process into host. The cell entry program is mediated by the spike proteins mainly by binding to the ACE-2 receptor in the host surface and subsequently mediate the viral infection. The major role played by spike proteins in host entry and attachment displays a wide possibility to be targeted to find effective vaccines and anti-bodies to neutralize the viral infection [6].

The Nsp9 replicase which is a non-structural protein is encoded by ORF1a which has no eminent function but is related with the viral RNA synthesis. This protein contains a single

folded beta-barrel which is unique unlike the single domain proteins. This fold is related to the OB-fold having a extended C-terminal in the subdomains of both SARS-CoV-2 3C-like protease that belongs to the serine protease superfamily. The crystal structure of Nsp9 replicase emphasises it as a dimeric protein. Nsp9 replicase specifically binds to the RNA further interacting with the nsp8 protein and activates the essential for its function [7]. As Nsp9 replicase a major role in viral replication it provides a hope for discovering novel drugs against this protein and thus inhibiting the viral progression.

As for now many of the vaccines and drugs are under clinical trials from across the globe. Drug repurposing has been the effective approach taken by the scientists across the globe to bring out an effective medicine for the eradication of the novel coronavirus. Anti-viral drugs such as chloroquine, hydroxychloroquine, which is used to treat malaria and arthritis was approved in USA to treat COVID-19 patients [8]. Some of the other drugs including remdesivir, actemra, galidesivir etc. are currently under clinical trial, but neither a single vaccine or therapeutic drugs are being currently approved by FDA to prevent or treat COVID-19 [9]. Therefore, structure-based drug repurposing through targeting Nsp9 replicase and Spike Proteins of SARS-CoV-2 would lead to the development of potential therapeutic approach against COVID-19.

Material and Methods

Data sources

In our study, a dataset of 2000 FDA approved compounds including antiviral, anti-malarial, anti-parasitic, anti-fungal, anti-tuberculosis and active phytochemicals from FDA and Indian Medicinal Plants, Phytochemistry and Therapeutic database were obtained [10, 11].

Preparation of receptor

125 The atomic coordinates of the protein crystal structure COVID-19, Nsp9 replicase (PDB ID-
126 6W4B), the spike protein (PDB ID-6LZG) were downloaded from the RCSB-PDB (protein
127 data bank) database. Prior to docking or analysis, the solvation parameters, charge assignment,
128 fragmental volumes and protein optimization was done using Autodock Tool 4 (ADT) [12, 13,
129 14].

130 **Preparation of ligands**

131 The 3D SDF structure of all the compounds were downloaded from PubChem database [15].
132 The 2D ligand structures of the compounds were designed using Chemdraw. The optimization
133 of the ligands was done using Avogadro and converted into PDB file format using Open Babel
134 software.

135 **Compound screening**

136 Molecular screening of the compounds was performed using PyRx virtual screening tool-
137 python prescription 0.8 software using Autodock wizard as the engine for molecular docking
138 [16, 17]. The ligands were minimized to their stable form. During the period of docking, the
139 protein was considered to be rigid and the ligands were considered to be flexible. Auto Grid
140 engine in PyRx was used to generate the configuration file for the grid parameters. The
141 application was also used to know/predict the amino acids in the active site of the protein that
142 interact with the ligands. The results less than 1.0Å in positional root-mean-square deviation
143 (RMSD) were considered ideal and clustered together for finding the favourable binding. The
144 highest binding energy (most negative) was considered as the ligand with maximum binding
145 affinity.

146 **Analysis and visualization**

147 Pymol version 2.3.4 and ADT were used for the visual analysis of the docking site and the
148 results were validated using Autodock-Vina [18].

149 **ADME analysis**

ADME analysis of the selected ligands obtained from PubChem was done on the basis of canonical SMILES using Swiss-ADME programme [19]. The ADME properties of the chosen compounds were calculated. The major ADME associated parameters such as Lipinski's rule of five, drug likeliness, pharmacokinetic properties, the solubility of the drug, were considered. The values of the observed properties are presented in Table 1 & 2.

Molecular dynamics & simulation

The complete study was performed on different modules of Schrodinger suite 2020-1 trial version. Both complexes were prepared prior to MD simulation in the protein preparation wizard and Prime module of Schrodinger suite to remove defects such as missing hydrogen atoms, incorrect bond order assignments, charge states, orientations of various groups and missing side chains suite [20-22]. Removal of steric clashes and strained bonds/angles were done by performing a restrained energy minimization, allowing movement in heavy atoms up to 0.3 Å. Extensive 50ns MD simulation was carried out for both complexes through Desmond, D. E. Shaw Research, New York, NY, 2015 [23] to access the binding stability of query molecule with respect to nelfinavir in the complex. Both complex systems were solvated in TIP3P water model and 0.15 M NaCl to mimic a physiological ionic concentration. The full system energy minimization step was done for 100ps. The MD simulation was run for 100ns at 300K temperature, standard pressure (1.01325 bar), within an orthorhombic box with buffer dimensions 10× 10× 10 Å³ and NPT ensemble. The energy (kcal/mol) was recorded at interval of 1.2 ps. The protein-ligand complex system was neutralized by balancing the net charge of the system by adding Na⁺ or Cl⁻ counter ions. The Nose-Hoover chain and Martyna-Tobias-Klein dynamic algorithm was used maintain the temperature of all the systems at 300 K and pressure 1.01325 bar, respectively.

Results and Discussion

Our study was focused on the drug repurposing against the Nsp9 replicase (PDB ID-6W4B) and the spike protein (PDB ID-6LZG) (Figure-1) of SARS-CoV-2 in combination as a potential therapeutic targets for the treatment of coronavirus. In this study, we have applied computational approach of structure based drug repurposing in combination in order to identify a specific therapeutic agent against SARS-CoV-2. We have created a database of 2000 FDA approved compounds including antiviral, anti-malarial, anti-parasitic, anti-fungal, anti-tuberculosis and active phytochemicals from FDA and Indian Medicinal Plants, Phytochemistry and Therapeutic database. The compounds were screened using a virtual screening tool PyRx, 15 hits were selected depending on their best binding energy. Further, molecular docking was performed for hits against Nsp9 replicase and the spike protein (Table 3 and 4).

Molecular docking is a computational approach which aims to identify non-covalent binding between (ligand/inhibitor) and protein (receptor). Docking predicts the mode of interaction between a receptor and the ligand for an established binding site. Binding energy suggests the affinity and strength of a specific ligand to which a compound binds and interacts at the active site pocket of a target protein. In order to understand the effect of active antiviral, anti-malarial, anti-parasitic, anti-fungal, anti-tuberculosis, anti-bacterial and active phytochemical compounds on COVID-19, molecular docking of 15 active compounds against each target selected after screening from PyRx, was performed. Further, based on their binding energy and best ADME properties, top three best compounds were selected.

Docking results of Nsp9 replicase with selected three compounds (Conivaptan, Telmisartan and Phaitanthrin D) showed best docking score and were found to be best molecules at the target site of the protein. Out of these, Conivaptan exhibited the best binding energy (-8.4 Kcal/mol) with Nsp9 replicase, interacting with CYS74, LEU107, LEU113, ALA108, LEU5, ASN34, LEU98, ASN96, LEU98, PHE41, THR36, ALA9, LEU104, VAL8,

200 ALA108, ASN99 and SER6 amino acid at the active site (Figure-3 A). Conivaptan was the
201 first of this class FDA approved arginine vasopressin antagonist for the management of
202 hypervolemic and euvolemic hyponatremia [24]. Telmisartan is an antagonist of angiotensin II
203 receptor which is highly selective for angiotensin II receptors type 1. It is a useful therapeutic
204 choice in the management of patients suffering from hypertension. Telmisartan exhibited (-8.1
205 Kcal/mol) binding affinity with Nsp9 replicase interacting with ARG100, LEU98, PHE9,
206 MET102, PHE41, ASN34, THR36, LEU113, LEU107, ALA108, VAL8, PRO7, LEU104,
207 PHE76, LEU5, GLU4, SER6, CYS74 and PHE91 amino acid residues (Figure-3 B).
208 Phaitanthrin D showed (-7.9 Kcal/mol) binding energy with Nsp9 replicase interacting with
209 6W4B. PHE76, CYS74, LEU89, LEU104, LEU107, GLY105, MET102, SER6, VAL8, PRO7,
210 ALA108 and LEU113 amino acid residues (Figure-3 C). Phaitanthrin D is natural alkaloid
211 found to exhibit potent anti-tubercular activity against MDR-TB [25]. The molecular docking
212 analysis in our study showed the inhibition potential of top three compounds against Nsp9
213 replicase ranked by binding energy and best ADME properties; Conivaptan > Telmisartan >
214 Phaitanthrin D.

215 Docking results of spike protein of SARS-CoV-2 with selected best three compounds
216 (Tegobuvir, Bromocriptine and Baicalin) showed best binding energy and were found to be
217 best molecules at the target site of the protein. Out of the 15 compounds, Tegobuvir exhibited
218 the binding energy (-8.1 Kcal/mol) interacting with PRO337, ALA344, ASN343, PHE342,
219 PHE347, PHE338, GLY339, GLU340 and VAL341 amino acid residues of spike protein
220 (Figure-4 A). Tegobuvir is a non-nucleoside inhibitor of hepatitis C virus (HCV) RNA
221 replication with proven antiviral activity in the patients suffering from chronic genotype 1 HCV
222 infection. Tegobuvir is an analog of imidazopyridine class inhibitors selectively targeting HCV
223 [26]. Bromocriptine functions as a serotonin modulator and postsynaptic dopamine receptor
224 clinically used to treat Parkinson's disease. Bromocriptine has also shown antiviral activity

against dengue virus replication [27]. Bromocriptine exhibited (-7.7 Kcal/mol) binding affinity with 6LZG. ASN450, LEU452, ILE468, TYR351, ALA352, SER349, LYS356, GLU340, ASN354, VAL341, THR345, ARG346, PHE347, ALA348 and SER349 amino acid residues of spike protein (Figure-4 B). Baicalin exhibited (-7.6 Kcal/mol) binding affinity interacting with 6LZG, ASN450, ARG346, ALA344, PHE342, GLU340, VAL341, SER399, ASN354, TRP353, ARG466, ILE468, ALA352, PHE400 and PHE347 amino acid residues of spike protein (Figure-4 C). Baicalin is a flavonoid derived from *Scutellaria baicalensis*. Baicalin has shown to exhibit a potent inhibitory activity against viruses such as anti-influenza virus and against chikungunya virus [28]. The molecular docking analysis showed best three compounds against spike protein of SARS-CoV-2 based on binding energy and ADME properties ranked; Tegobuvir > Bromocriptine > Baicalin.

In addition to the selected three best compounds against the spike protein, conivaptan (-7.4 Kcal/mol), Phaitanthrin D (-7.2 Kcal/mol) and Telmisartan (-7.2 Kcal/mol) also exhibited good docking score against the spike protein suggesting that these compounds could potentially target both Nsp9 replicase as well as the spike protein.

Molecular dynamics study of Conivaptan with Nsp9 replicase (Figure-5) and Tegobuvir with spike protein (Figure-6) for 50 ns showed strong interaction between protein and ligand and stability of ligand at the active domain of proteins interacting through water bridges, hydrophobic interactions, H-bond. The molecular dynamic study strongly validates the molecular docking data of protein ligand interaction.

The major criteria to evaluate the likeliness of the drug is “Lipinski’s rule of five” suggesting if a specific ligand with a certain pharmacological and biological activity has chemical and physical properties that would make it as a chosen option for orally active drug for humans. Lipinski’s rule suggests the molecular properties that are crucial for pharmacokinetics of a drug in the human body for example; absorption, distribution,

metabolism, and excretion (ADME). In Lipinski's rule of five, three or more than 3 violations do not follow the rule of drug likeliness and is not considered in order to proceed further with the drug discovery approach. ADME studies of selected 15 compounds showed that out of 15, all virtual hits were successful at passing through these test filters of ADME.

Conclusion

In view of the current outbreak of coronavirus and rising death toll scenario, novel drug discovery is a challenge constrained by time, but on the other hand, drug repurposing could be a great help in the development of therapeutic drugs and the effective management of COVID-19. Structure-based drug design approaches have developed into valuable drug discovery tools, owing to their synergy and versatility. Here, we have described the structure based drug repurposing from a collection of FDA approved antiviral, anti-malarial, anti-parasitic, anti-fungal, anti-tuberculosis and active phytochemicals compounds against Nsp9 replicase and spike protein of SARS-CoV-2. Several molecules were identified as potent inhibitors of Nsp9 replicase (Conivaptan, Telmisartan and Phaitanthrin D), spike protein (Tegobuvir, Bromocriptine, and Baicalin) of SARS-CoV-2. Interestingly, the compounds such as Conivaptan, Phaitanthrin D and Telmisartan showed good binding affinity with both Nsp9 replicase and the spike protein suggesting the potential of these compounds to inhibit multiple targets of SARS-CoV-2. Therefore, we suggest that these compounds might be applicable in the management of COVID-19 and can be proposed as potential lead compounds for multi-targeted drug development against SARS-CoV-2. Further, *in vitro* and *in vivo* validation of these studies would lead to the development of therapeutic strategies through targeting Nsp9 replicase and spike protein of SARS-CoV-2.

Acknowledgements

Authors acknowledge Department of Science and Technology-Science and Engineering Research Board (DST- SERB), Government of India for partial financial support.

Conflict of Interest

Authors declare no conflict of Interest

References

- [1] A. R. Fehr and S. Perlman, "Coronaviruses: An overview of their replication and pathogenesis," in *Coronaviruses: Methods and Protocols*, 2015.
- [2] D. Schoeman and B. C. Fielding, "Coronavirus envelope protein: Current knowledge," *Virology Journal*. 2019.
- [3] C. Huang *et al.*, "Clinical features of patients infected with 2019 novel coronavirus in Wuhan, China," *Lancet*, 2020.
- [4] D. Muriaux and J. L. Darlix, "Properties and functions of the nucleocapsid protein in virus assembly," *RNA Biology*. 2010,.
- [5] K. P. Lim, L. F. P. Ng, and D. X. Liu, "Identification of a Novel Cleavage Activity of the First Papain-Like Proteinase Domain Encoded by Open Reading Frame 1a of the Coronavirus Avian Infectious Bronchitis Virus and Characterization of the Cleavage Products," *J. Virol.*, 2000.
- [6] F. Li. " Structure, Function, and Evolution of Coronavirus Spike Proteins." *Annual Rev Virol*. 2016, 3(1), 237-261.
- [7] G. Sutton et al. "The nsp9 Replicase Protein of SARS-coronavirus, Structure and Functional Insights." *Structure*. 2004, 12(2), 341-53.
- [8] F. Touret and X. de Lamballerie, "Of chloroquine and COVID-19," *Antiviral Research*. 2020.
- [9] "<https://www.cdc.gov/coronavirus/2019-ncov/hcp/therapeutic-options.html>."
- [10] S. Choudhuri, J.A. Symons, J. Deval, "Innovation and trends in the development and approval of antiviral medicines:1987-2017 and beyond." *Antiviral res.*,2018.
- [11] K. Mohanraj, B. Shanmugun, R.P. Vivel-ananth, R.P. Bharath Chand, S.R. Aparna, P. Mangalapandi, A. Samal, "IMPAAT: A curated database of Indian Medicinal Plants, Phytochemistry, And Therapeutics." *Sci rep*. 2018.
- [12] G. Morris, R. Huey, W. Lindstrom, et al. AutoDock4 and AutoDockTools4: Automated docking with selective receptor flexibility. *J. Comput. Chem*. 2009.
- [13] V. Chandel, M. Srivastava, A. Srivastava, S. Asthana, D. Kumar "In-silico interactions of active Phytochemicals with c-Myc EGFR and ERBB2 oncoproteins." *Chemical Biology Letters*. 2020, 7(1), 47-54.
- [14] D. Kumar, V. Chandel, S.Raj, B.Rathi " *In silico* identification of potent FDA approved drugs against Coronavirus COVID-19 main protease: A drug repurposing approach." *Chemical Biology Letters.*, 2020, 7(3), 166-175.
- [15] N.M. O'Boyle, M. Banck, C.A. James, et al. Open Babel: An Open chemical toolbox. *J. Cheminform*. 2011.

- [16] S. Dallakyan, A.J. Olson. " Small-molecule library screening by docking with PyRx." Methods mol biol. 2015.
- [17] N.S. Pagadala, K. Syed, T. Jack." Software for molecular docking : a review." Biophys Rev. 2017.
- [18] D. Seeliger, B.L.De. Groot. " Ligand docking and binding site analysis with PyMOL and Autodock/vina." J Comput Aided Mol Des." 2010
- [19] A. Diana, O. Michielin, V.Zoete." SwissADME: a free web tool to evaluate pharmacokinetics, drug- likeness and medicinal chemistry friendliness of small molecules." Sci rep. 2017.
- [20] Schrödinger Release 2020-1: Maestro, Schrödinger, LLC, New York, NY, 2020.
- [21] Schrödinger Release 2020-1: Protein Preparation Wizard; Epik, Schrödinger, LLC, New York, NY, 2016; Impact, Schrödinger, LLC, New York, NY, 2016; Prime, Schrödinger, LLC, New York, NY, 2020
- [22] Schrödinger Release 2020-1: Prime, Schrödinger, LLC, New York, NY, 2020
- [23] Schrödinger Release 2020-1: Desmond Molecular Dynamics System, D. E. Shaw Research, New York, NY, 2020. Maestro-Desmond Interoperability Tools, Schrödinger, New York, NY, 2020
- [24] J.K. Ghali, J.O. Farah, S. Daifallah, H.A.Zabalawi, H.D. Zimmy." Conivaptan and its role in the treatment of hyponatremia." Drug Des Develop. Ther. 2009
- [25] A. Kamal, B.V. Reddy, B. Sridevi, A. Rajkumar, A. Venkateswarlu, G.Sravanthi, J.P. Sridevi, P.Yogeshwari, D.Sriram. " Synthesis and biological evaluation of phaitanthrin congeners as anti-mycobacterial agents." Bioorg Med Chem Lett. 2015
- [26] I. Vliegen, J. Paeshuyse, W. Zhong, J. Neyts. " In vitro combinations containing Tegobuvir are highly efficient in curing cells from HCV replicon and in delaying/preventing the development of drug resistance." Antiviral Res. 2015.
- [27] F. Kato, Y. Ishida, S. Oishi et al. " Novel antiviral activity of bromocriptine against dengue virus replication." Antiviral Res. 2016.
- [28] M. Chu, L. Xu, M. Zhang, Z. Chu, Y.D. Wang. "Role of Baicalin in Anti-Influenza Virus A as a Potent Inducer of IFN-Gamma." Biomed Research International. 2014

Figure Legends

Figure-1: Crystal structure of protein/receptor (A) Nsp9 replicase (PDB ID-6W4B) of SARS-CoV-2. The structure is shown in ribbon representation, coloured from the N-terminus to the C-terminus with colours changing from blue through green and yellow to red. (B) Spike protein (PDB ID-6LZG) of SARS-CoV-2 shows ribbon structure representation, coloured from the N-terminus to the C-terminus with colours changing from red through yellow and green to blue Ribbon structure.

Figure-2: Docking analysis and visualisation of protein-ligand complex (A) Nsp9 replicase (pink) and Conivaptan (yellow), (B) Nsp9 replicase (pink) and Telmisartan (green), (C) Nsp9 replicase (pink) and Phaitanthrin D (salmon), (D) Spike protein (green) and Tegobuvir (pink), (E) Spike protein (green) and Bromocriptine (blue), (F) Spike protein (green) and Baicalin (orange). The binding site of the Nsp9 replicase and spike protein is depicted using surface representation. The ligands are depicted using stick model representation. The ligand is interacting at the active site pocket of the protein/receptor.

Figure-3: Figure shows interaction between the active site residues of the Nsp9 replicase protein and ligands with their respective binding energies. (A) Nsp9 replicase (green) with conivaptan (carbon in gray) (Binding energy -8.4 Kcal/mol), (B) Nsp9 replicase (hot-pink) with Telmisartan (carbon in green) (Binding energy -8.1 Kcal/mol), (C) Nsp9 replicase (yellow) with Phaitanthrin D (carbon in dark pink) (Binding energy -7.9 Kcal/mol). The protein backbone is depicted using ribbon structure representation and ligands are depicted using stick model representation. Bond length is depicted in Angstrom. Figure represents strong binding affinity between the hydrophobic pocket of the protein and ligand.

Figure-4: Figure shows interaction between the active site residues of the spike protein and ligands with their respective binding energies. (A) Spike protein (purple) with Tegobuvir (carbon in yellow) (Binding energy -8.1 Kcal/mol), (B) Spike protein (wheat) with Bromocriptine (carbon in light-blue) (Binding energy -7.7 Kcal/mol), (C) Spike protein (grey) with Baicalin (carbon in light-green) (Binding energy -7.6 Kcal/mol). The protein backbone is depicted using ribbon structure representation and ligands are depicted using stick model representation. Bond length is depicted in Angstrom. Figure represents strong binding affinity between the hydrophobic pocket of the protein and ligand.

Figure-5: Molecular dynamics and simulation of Conivaptan with Nsp9 replicase complex. (A) Ramachandran plot of Conivaptan-Nsp9 replicase complex represents 102 (95.2%) residues lie in favoured region 4 (3.7%) residues lie in allowed region and 1 (0.9%) outlier residues. (B) RMSD plot for C α of Nsp9 replicase in complex with Conivaptan. (C) RMSF plot of residue number and C-alpha of Nsp9 replicase at 50 ns simulation. It predicts the fluctuations of the C-alpha atoms; Residues are shown in three letter code with their respective number in green color belong to binding site residues interacting to compound shown in green line. (D) A timeline representation of the interactions and contacts (H-bonds, hydrophobic, ionic, water bridges) with compound. The top panel shows the total number of specific contacts the protein makes with the ligand over the course of the trajectory. The bottom panel shows which residues interact with the ligand in each trajectory frame.

Figure-6: Molecular dynamics and simulation of Tegobuvir with spike protein complex. (A) Ramachandran plot of Tegobuvir-spike protein complex represents 179 (92.7%) residues lie in favoured region 13 (6.7%) residues lie in allowed region and 1 (0.5%) outlier residues. (B) RMSD plot for C α of spike protein in complex with Tegobuvir. (C) RMSF plot of residue number and C-alpha of spike protein at 50 ns simulation. It predicts the fluctuations of the C-alpha atoms; Residues are shown in three letter code with their respective number in green color belong to binding site residues interacting to compound shown in green line. (D) A timeline representation of the interactions and contacts (H-bonds, hydrophobic, ionic, water bridges) with compound. The top panel shows the total number of specific contacts the protein makes with the ligand over the course of the trajectory. The bottom panel shows which residues interact with the ligand in each trajectory frame.

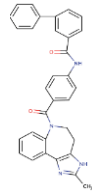
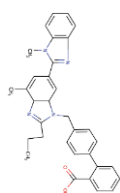
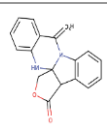
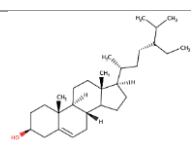
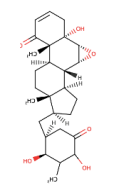
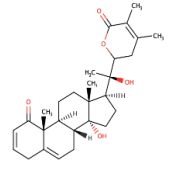
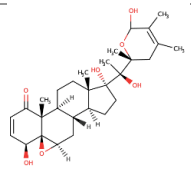

Table-1: Molecular docking analysis of antiviral compounds against Nsp9 replicase (6W4B) of SARS-CoV-2.

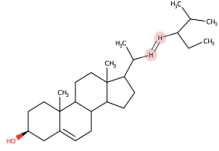
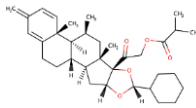
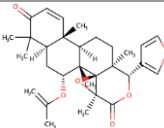
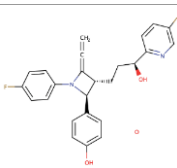
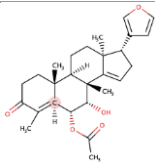
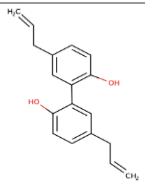
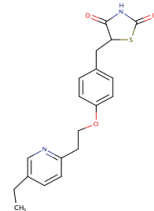
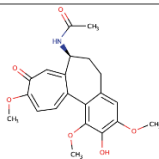
Protein	Compound	Binding Energy (Kcal/mol)	Amino acid residues
Nsp9 replicase	Conivaptan	-8.4	CYS74, LEU107, LEU113, ALA108, LEU5, ASN34, ASN96, LEU98, PHE41, THR36, ALA9, LEU104, VAL8, ASN99, SER6
	Telmisatan	-8.1	ARG100, LEU98, PHE9, MET102, PHE41, ASN34, THR36, LEU113, LEU107, ALA108, VAL8, PRO7, LEU104, PHE76, LEU5, GLU4, SER6, CYS74, PHE91
	Phaitanthrin D	-7.9	PHE76, CYS74, LEU89, LEU104, LEU107, GLY105, MET102, SER6, VAL8, PRO7, ALA108, LEU113
	Phytosterols	-7.8	PHE41, THR36, ASN34, ASN99, SER6, VAL8, LEU5, CYS74, PHE76, LEU89, LEU104, MET102, LEU113, ALA108, LEU107,
	Withanolide R	-7.8	PHE76, CYS74, LEU89, PHE91, VAL103, MET102, ASN99, GLN105, LEU104, LEU107, PHE41, ASN34, THR36, LEU113, LEU5, VAL8, ALA108
	Withanolide G	-7.7	ASN96, ASN99, MET102, LEU98, LEU104, ALA108, PHE41, ASN34, VAL8, LEU113, LEU5, CYS74, THR36, SER6
	17-alpha-hydroxywithanolide D	-7.7	GLU4, PHE76, LEU5, SER6, PRO7, LEU113, LEU107, ALA108, LEU104, VAL8, ALA9, MET102, ASN34, LEU98, ALA99, PHE41
	Stigmasta-5, 22-dien-3-ol	-7.7	PHE41, ASN96, ASN99, ASN34, VAL8, LEU5, LEU113, PHE76, LEU107, LEU89, CYS74, ALA108, MET102, SER6
	Gedunin	-7.6	THR36, ASN34, LEU113, VAL8, ALA108, SER6, LEU5, GLU4, CYS74, LEU107, MET102, ASN99, LEU98, LEU104
	Ciclesonide	-7.5	LEU113, SER6, LEU5, GLU4, ASN3, CYS7, VAL8, THR36, THR35, ASN34, ALA108, PHE41, MET102, ASN99, LEU98, PHE91, ASN100,
	Ezetimibe	-7.5	ASN34, MET102, LEU104, PHE91, GLY105, ASN3, CYS74, LEU89, PHE76, SER6, LEU113, PRO7, VAL8, ALA108, ALA9,
	Meldenin	-7.5	ASN99, MET102, PHE41, THR36, SER6, VAL8, LEU113, LEU107, ALA108, THR35, LEU5
	Magnolol	-7.4	MET102, GLY105, ARG100, LEU104, LEU107, ALA108, PHE91, LEU89, CYS74, PHE76, SER6, LEU113, VAL8, PRO7
	Pioglitazone	-7.4	MET102, ASN99, ASN34, ALA108, LEU104, LEU107, LEU113, LEU85, VAL8, THR36, PHE41, THR35, SER6,
	Gloriosine	-7.4	LYS102, PHE103, VAL104, ARG105, ILE106, GLN107, GLN110, PHE294, PHE8, ASN151, TYR154, ASP153

Table-2: Molecular docking analysis of antiviral compounds against spike protein (6LZG) of SARS-CoV-2.

Protein	Compound	Binding Energy (Kcal/mol)	Amino acid residues
Spike Protein	Tegobuvir	-8.1	PRO337, ALA344, ASN343, PHE342, PHE347, PHE338, GLY339, GLU340, VAL341
	Bromocriptine	-7.7	ASN450, LEU452, ILE468, TYR351, ALA352, SER349, LYS356, GLU340, ASN354, VAL341, THR345, ARG346, PHE347, ALA348, SER349
	Baicalin	-7.6	ASN450, ARG346, ALA344, PHE342, GLU340, VAL341, SER399, ASN354, TRP353, ARG466, ILE468, ALA352, PHE400, PHE347
	Deleobuvir	-7.6	ARG466, TRP353, ASN354, PRO463, PHE464, PRO426, TYR396, GLU516, ARG355
	Dantrolene	-7.6	TYR351, ALA352, ASN354, SER399, LYS356, ALA348, SER349, LEU452, ASN450, ARG346, PHE347, ALA344, VAL341, PHE342, GLU340
	Cassameridine	-7.4	ARG355, PHE464, PRO463, TYR396, GLU516, SER514, PRO426, PHE515, PHE429, ASP428, PRO426
	Chrysin-7-O-glucuronide	-7.4	LYS356, ASN354, ALA352, TYR351, SER349, ASN450, ARG346, ALA344, GLU340, PHE347, ALA348, PHE400, SER399, VAL341
	Conivaptan	-7.4	PHE464, GLU465, ARG466, ARG355, ASN354, TRP353, ALA352
	Phaitanthrin D	-7.2	PRO463, PHE464, ARG355, TYR396, SER514, THR430, PHE515, GLU516
	Telmisartan	-7.2	ILE468, ARG466, ASN354, PHE347, ARG346, ALA352, ARG355, LYS356, TYR396, ARG357
	Troglitazone	-7.2	ARG466, GLU465, PRO463, PHE464, TRP353, ARG355, PRO426, ASP428, PHE429, THR430, SER514, TYR396, PHE515, GLU516
	Raltegravir	-7.1	ALA352, SER349, ALA348, PHE347, ASN354, SER399, ARG346, ALA344, GLU340, VAL341, ARG357, LYS356, ARG355
	Ceferoperazone	-7.1	LEU452, TYR451, ASN450, SER349, ARG346, PHE347, ALA344, ALA352, TRP353, SER399, ASN354, VAL341, GLU340, ARG355, LYS356, ARG477, PHE347, ALA344
	Dasatinib	-7.0	ARG357, LYS356, TYR396, ARG355, ARG346, PHE347, ALA348, ASN450, TYR451, SER349, ALA332, TYR351, ILE468, ARG466, TRP353, ASN354, SER349
	Dolutegravir	-7.0	ARG355, TYR396, PHE515, SER514, GLU516, THR430, PHE429, PRO426, PRO463, GLU465, ARG466, TRP353, PHE464

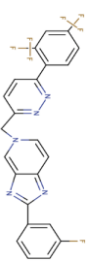
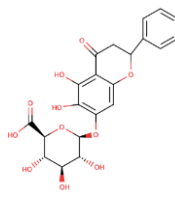
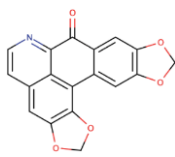
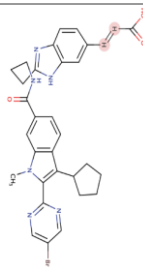

Table-3: ADME Properties of selected inhibitors of Nsp9 replicase.

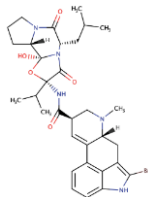
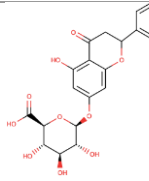
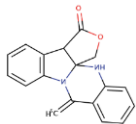

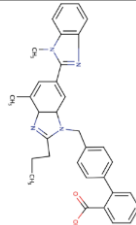
S. No	Compound	Molecular formula	ADME Properties (Lipinki's Rule of Five)		Structure	Drug likeness
			Properties	Value		
1.	Conivaptan	$C_{32}H_{26}N_4O_2$	Molecular weight (<500Da)	498.57		Yes
			LogP (<5)	5		
			H-Bond donor (5)	2		
			H-bond acceptor (<10)	3		
			Violations	0		
2.	Telmisartan	$C_{33}H_{30}N_4O_2$	Molecular weight (<500Da)	514.62		Yes
			LogP (<5)	5.9		
			H-Bond donor (5)	1		
			H-bond acceptor (<10)	4		
			Violations	2		
3.	Pharanthrin D	$C_{17}H_{12}N_2O_3$	Molecular weight (<500Da)	292.29		Yes
			LogP (<5)	1.7		
			H-Bond donor (5)	1		
			H-bond acceptor (<10)	3		
			Violations	0		
4.	Phytosterols	$C_{29}H_{50}O$	Molecular weight (<500Da)	414.71		Yes
			LogP (<5)	7.1		
			H-Bond donor (5)	1		
			H-bond acceptor (<10)	1		
			Violations	1		
5.	Withanolide R	$C_{28}H_{38}O_6$	Molecular weight (<500Da)	454.60		Yes
			LogP (<5)	3.9		
			H-Bond donor (5)	2		
			H-bond acceptor (<10)	5		
			Violations	0		
6.	Withanolide G	$C_{28}H_{38}O_5$	Molecular weight (<500Da)	480.64		Yes
			LogP (<5)	4.1		
			H-Bond donor (5)	1		
			H-bond acceptor (<10)	6		
			Violations	0		
7.	17-alpha-hydroxywithanolide D	$C_{28}H_{40}O_7$	Molecular weight (<500Da)	488.61		Yes
			LogP (<5)	2.1		
			H-Bond donor (5)	4		
			H-bond acceptor (<10)	7		
			Violations	0		
8	Stigmasta-5,22-dien-3-ol	$C_{29}H_{48}O$	Molecular weight (<500Da)	412.69		Yes
			LogP (<5)	6.9		
			H-Bond donor (5)	1		

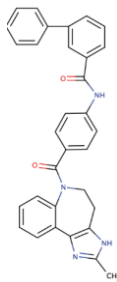
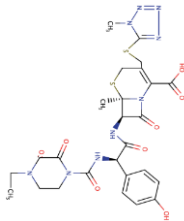
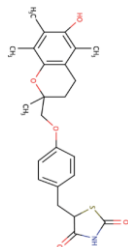
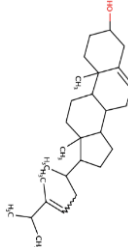
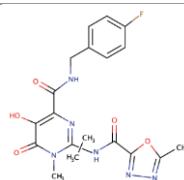
			H-bond acceptor (<10)	1		
			Violations	1		
9.	Gedunin	C ₂₈ H ₃₄ O ₇	Molecular weight (<500Da)	482.57		Yes
			LogP (<5)	3.7		
			H-Bond donor (5)	0		
			H-bond acceptor (<10)	7		
			Violations	0		
10.	Ciclesonide	C ₃₂ H ₄₄ O ₇	Molecular weight (<500Da)	540.69		Yes
			LogP (<5)	4.4		
			H-Bond donor (5)	1		
			H-bond acceptor (<10)	7		
			Violations	1		
11.	Ezetimibe	C ₂₄ H ₂₁ F ₂ NO ₃	Molecular weight (<500Da)	409.43		Yes
			LogP (<5)	4.3		
			H-Bond donor (5)	2		
			H-bond acceptor (<10)	5		
			Violations	1		
12	Meldenin	C ₂₈ H ₃₈ O ₅	Molecular weight (<500Da)	454.60		Yes
			LogP (<5)	4.4		
			H-Bond donor (5)	1		
			H-bond acceptor (<10)	5		
			Violations	0		
13	Magnolol	C ₁₈ H ₁₈ O ₂	Molecular weight (<500Da)	266.33		Yes
			LogP (<5)	4.2		
			H-Bond donor (5)	2		
			H-bond acceptor (<10)	5		
			Violations	0		
14	Pioglitazone	C ₁₉ H ₂₀ N ₂ O ₃ S	Molecular weight (<500Da)	356.44		Yes
			LogP (<5)	3.1		
			H-Bond donor (5)	1		
			H-bond acceptor (<10)	4		
			Violations	0		
15.	Gloriosine	C ₂₁ H ₂₃ NO ₆	Molecular weight (<500Da)	385.41		Yes
			LogP (<5)	2.1		
			H-Bond donor (5)	1		
			H-bond acceptor (<10)	6		
			Violations	0		

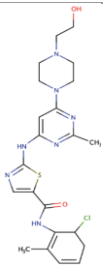
457
458
459
460
461
462

Table-4: ADME Properties of selected inhibitors of spike protein

S. No	Compound	Molecular formula	ADME Properties (Lipinki's Rule of Five)		Structure	Drug likeliness
			Properties	Value		
1.	Tegobuvir	$C_{25}H_{14}F_7N_5$	Molecular weight (<500Da)	517.40		Yes
			LogP (<5)	5.8		
			H-Bond donor (5)	0		
			H-bond acceptor (<10)	11		
			Violations	2		
2.	Baicalin	$C_{21}H_{18}O_{11}$	Molecular weight (<500Da)	446.36		Yes
			LogP (<5)	0.2		
			H-Bond donor (5)	6		
			H-bond acceptor (<10)	11		
			Violations	2		
3.	Cassameridine	$C_{18}H_{19}NO_5$	Molecular weight (<500Da)	319.27		Yes
			LogP (<5)	2.7		
			H-Bond donor (5)	0		
			H-bond acceptor (<10)	6		
			Violations	0		
4.	Deleobuvir	$C_{34}H_{33}BrN_6O_3$	Molecular weight (<500Da)	653.57		Yes
			LogP (<5)	5.1		
			H-Bond donor (5)	2		
			H-bond acceptor (<10)	6		
			Violations	1		
5.	Bromocriptine	$C_{32}H_{40}BrN_5O_5$	Molecular weight (<500Da)	654.59		Yes
			LogP (<5)	3.1		
			H-Bond donor (5)	3		

			H-bond acceptor (<10)	6		
			Violations	1		
6.	Chrysin-7-O-glucuronide	$C_{21}H_{18}O_{10}$	Molecular weight (<500Da)	430.36		Yes
			LogP (<5)	0.64		
			H-Bond donor (5)	5		
			H-bond acceptor (<10)	10		
			Violations	0		
7.	Phaethanthrin D	$C_{29}H_{48}O$	Molecular weight (<500Da)	412.69		Yes
			LogP (<5)	6.9		
			H-Bond donor (5)	1		
			H-bond acceptor (<10)	1		
			Violations	1		
8	Dantrolene	$C_{14}H_{10}N_4O_5$	Molecular weight (<500Da)	314.25		Yes
			LogP (<5)	0.72		
			H-Bond donor (5)	1		
			H-bond acceptor (<10)	4		
			Violations	0		
9.	Telmisartan	$C_{24}H_{21}F_2NO_3$	Molecular weight (<500Da)	409.43		Yes
			LogP (<5)	4.3		
			H-Bond donor (5)	2		
			H-bond acceptor (<10)	5		
			Violations	1		
10	Conivaptan	$C_{28}H_{38}O_5$	Molecular weight (<500Da)	454.60		Yes
			LogP (<5)	4.4		
			H-Bond donor (5)	1		

			H-bond acceptor (<10)	5		
			Violations	0		
11	Cefoperazone	$C_{18}H_{18}O_2$	Molecular weight (<500Da)	266.33		Yes
			LogP (<5)	4.2		
			H-Bond donor (5)	2		
			H-bond acceptor (<10)	5		
			Violations	0		
12	Troglitazone	$C_{24}H_{27}NO_5$	Molecular weight (<500Da)	441.54		Yes
			LogP (<5)	4.1		
			H-Bond donor (5)	2		
			H-bond acceptor (<10)	5		
			Violations	0		
13	Dolutegravir	$C_{20}H_{19}F_2N_3O_5$	Molecular weight (<500Da)	419.38		Yes
			LogP (<5)	1.8		
			H-Bond donor (5)	2		
			H-bond acceptor (<10)	7		
			Violations	0		
14	Raltegravir	$C_{20}H_{21}FN_6O_5$	Molecular weight (<500Da)	444.42		Yes
			LogP (<5)	1.4		
			H-Bond donor (5)	3		
			H-bond acceptor (<10)	9		
			Violations	1		
15	Dasatinib	$C_{22}H_{26}ClN_7O_2S$	Molecular weight (<500Da)	488.01		Yes
			LogP (<5)	2.8		
			H-Bond donor (5)	3		

			H-bond acceptor (<10)	6		
			Violations	0		

465

466

Figure-1

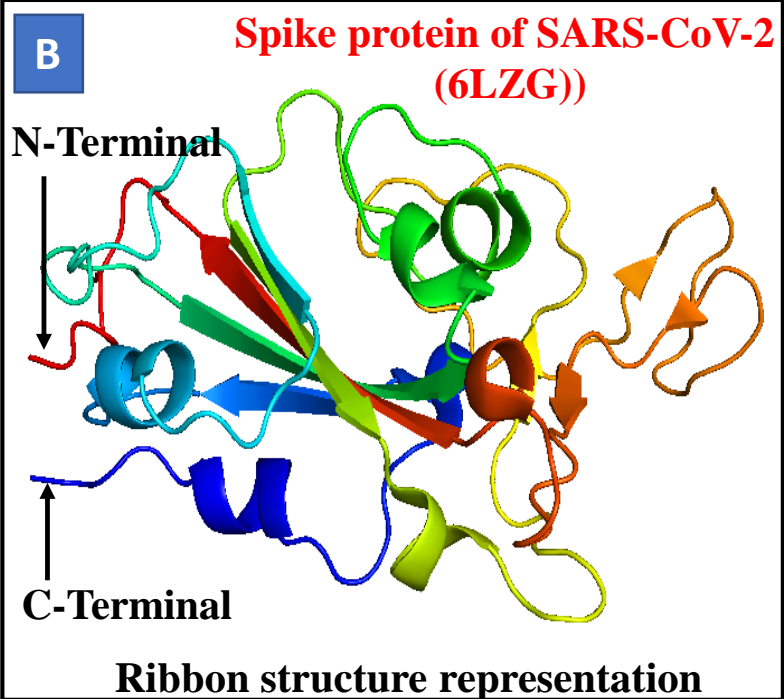
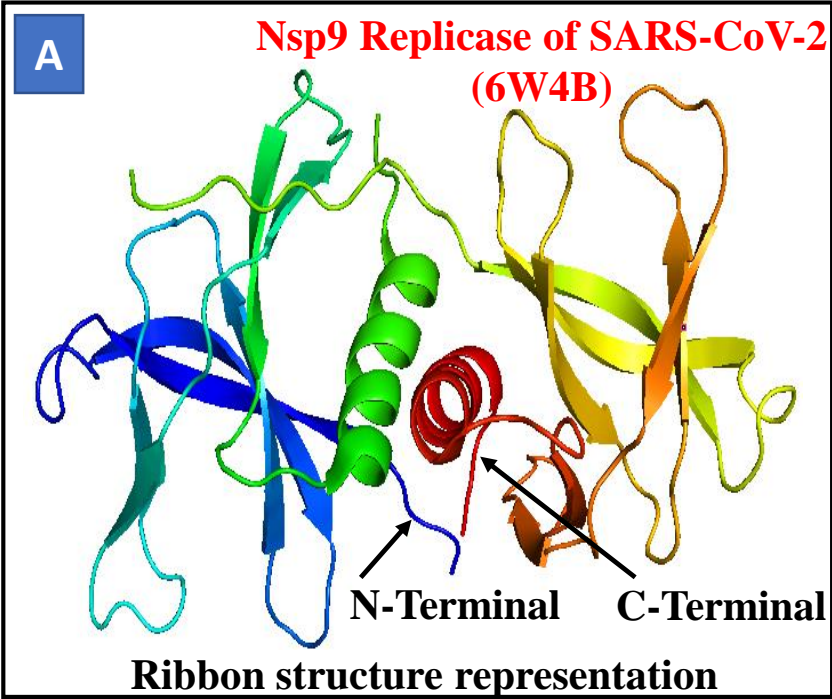


Figure-2

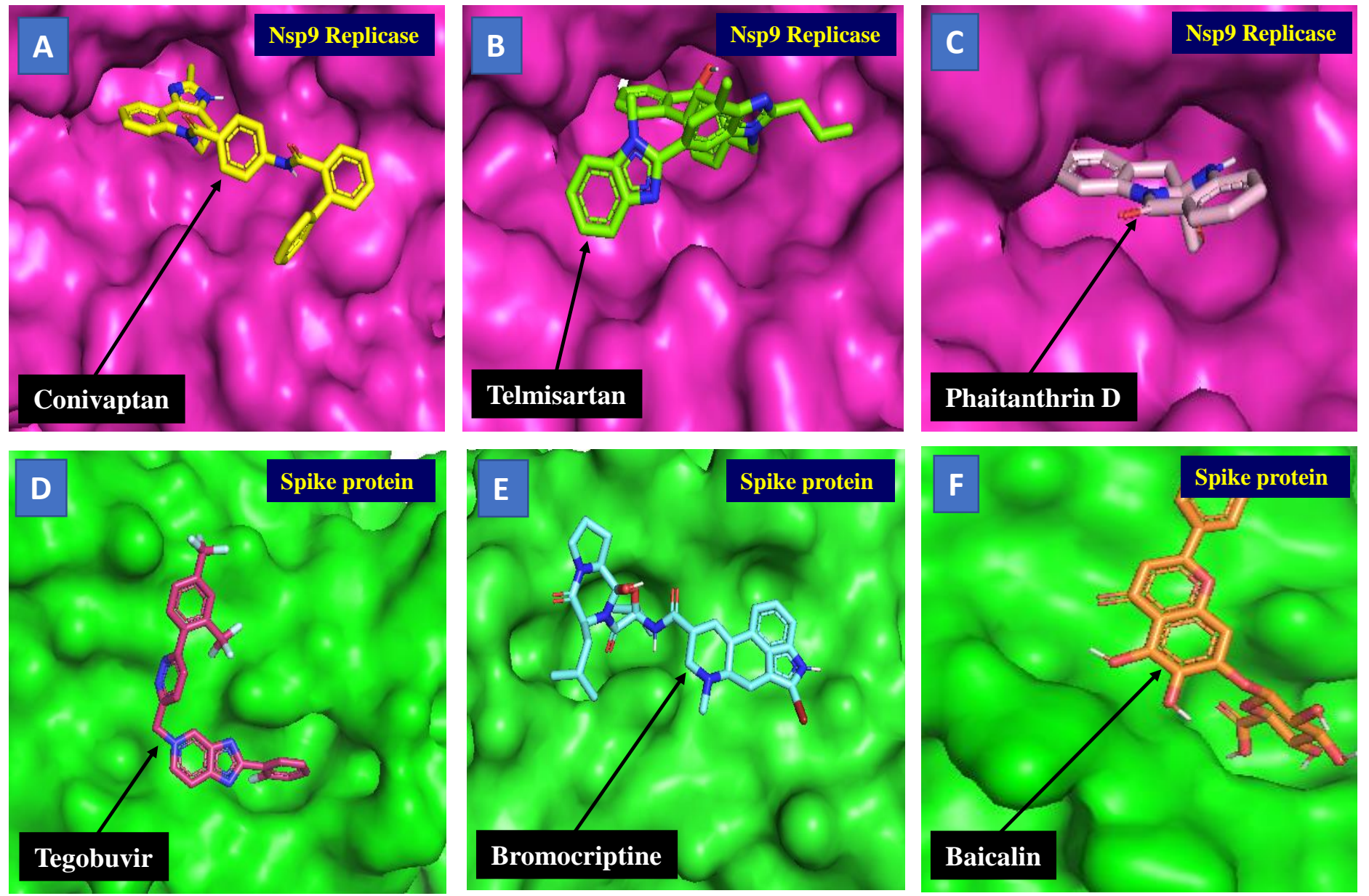


Figure-3

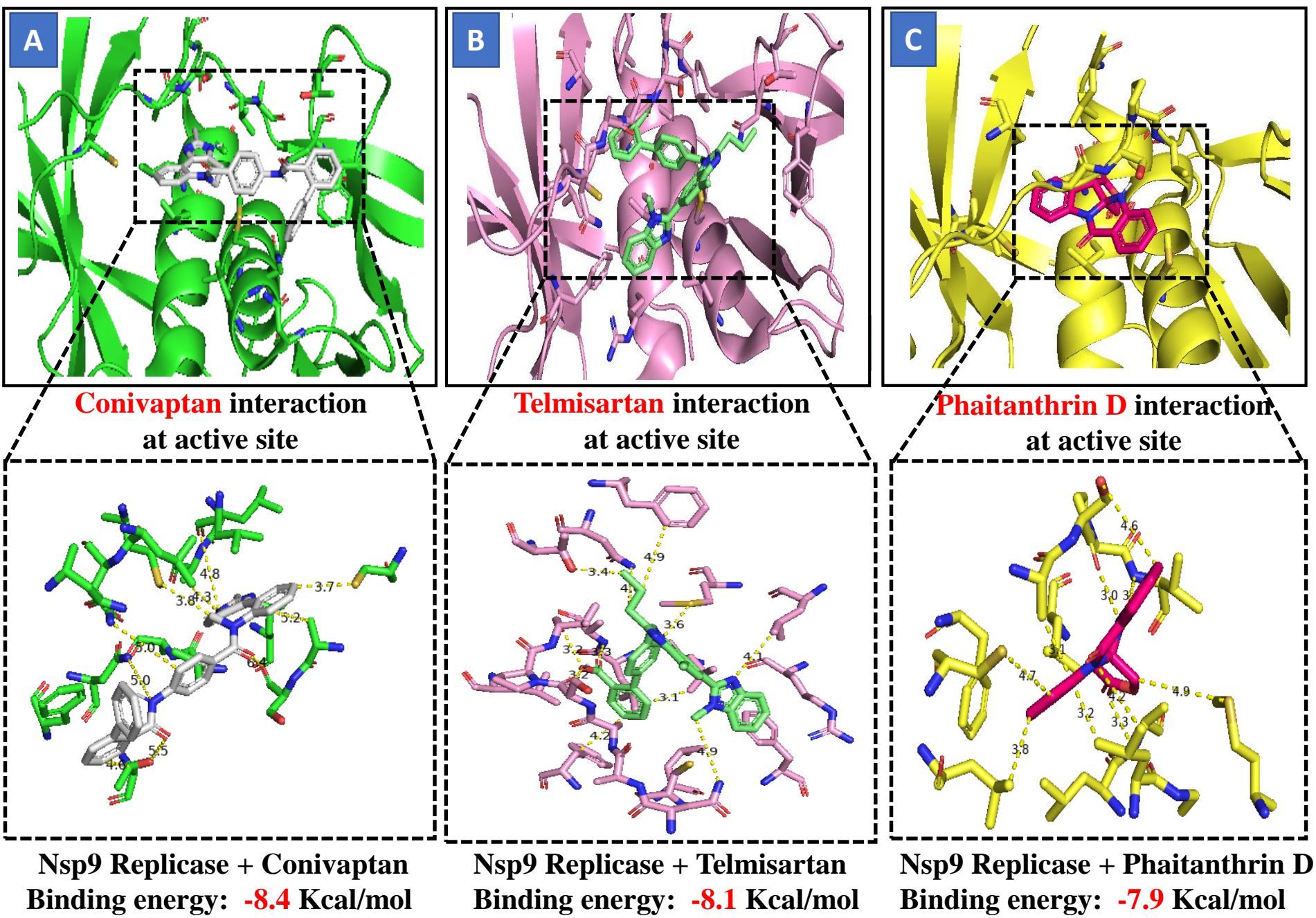


Figure-4

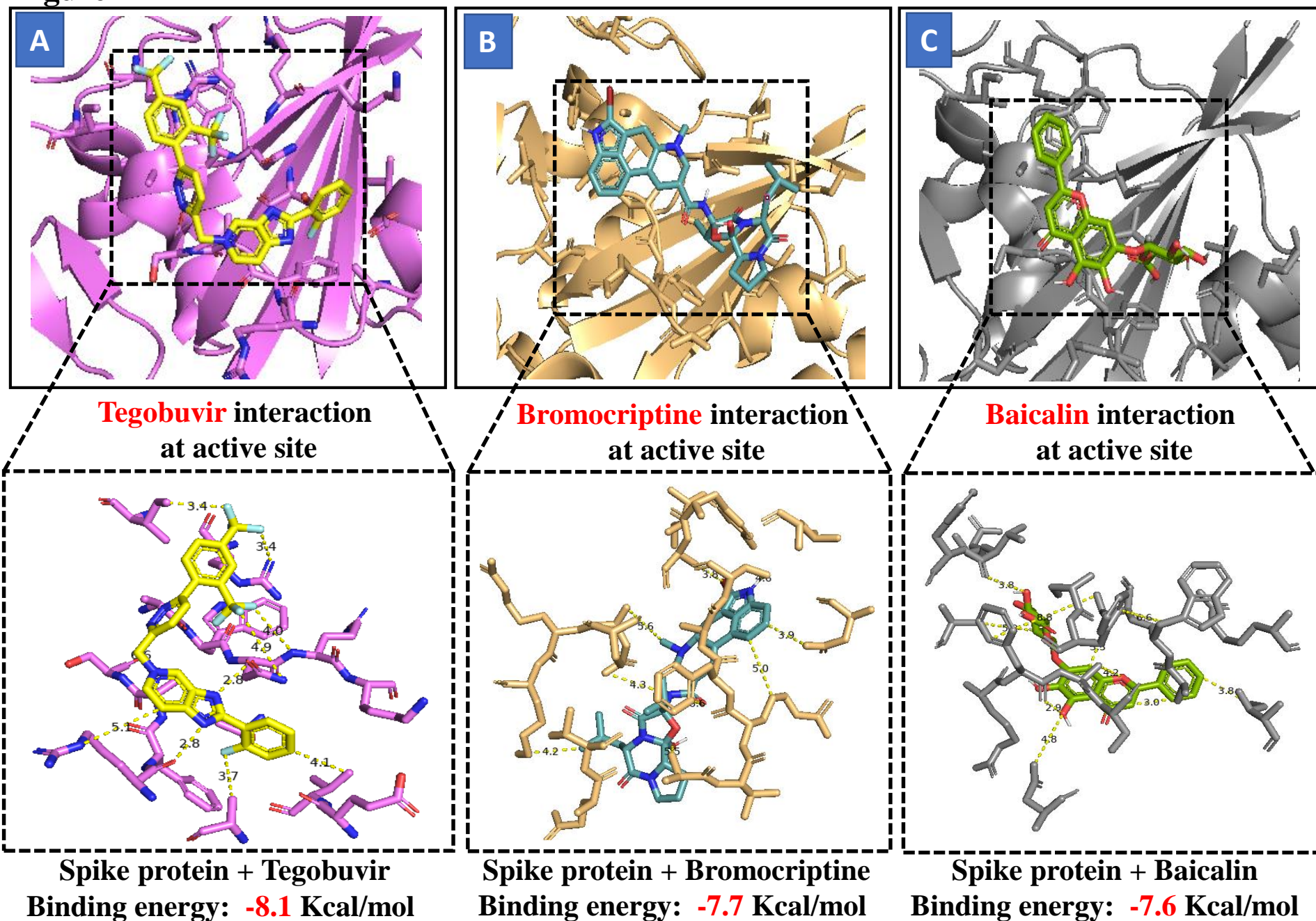


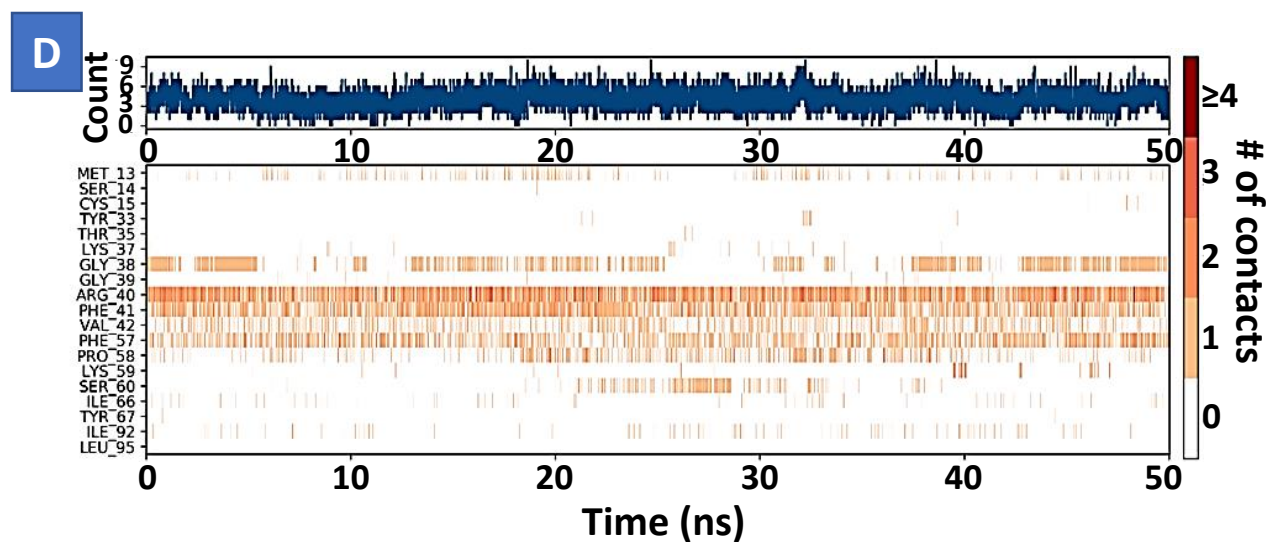
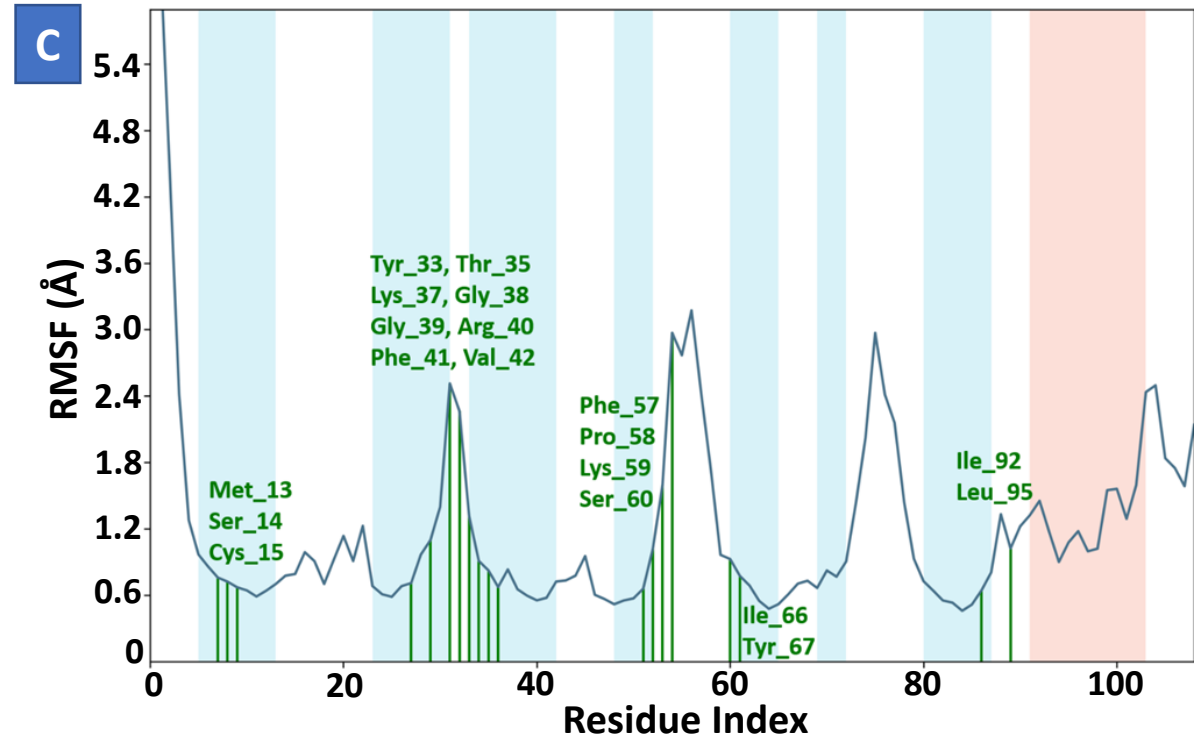
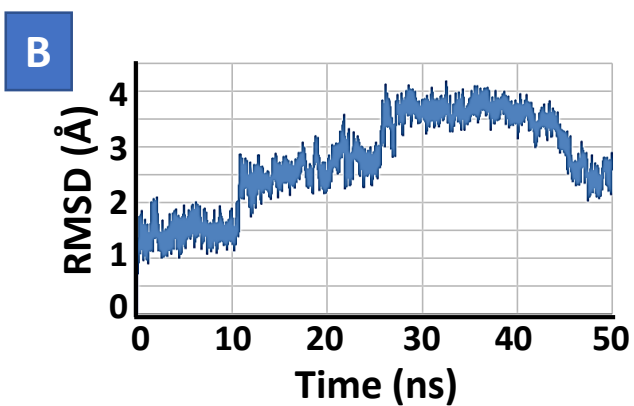
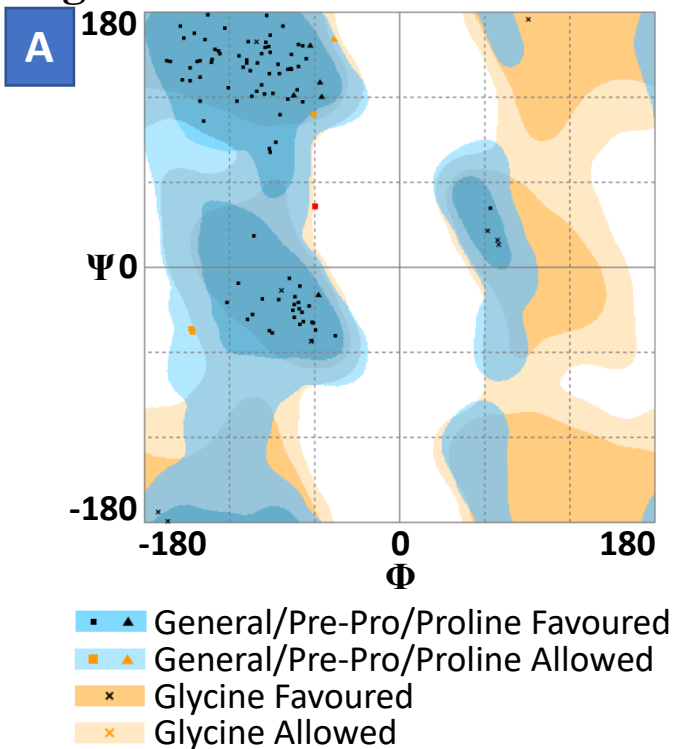
Figure-5

Figure-6